Regulatory T cells actively infiltrate metastatic brain tumors

ADAM QUASAR SUGIHARA, CLEO E. ROLLE and MACIEJ S. LESNIAK

The Brain Tumor Center, The University of Chicago, Chicago, IL 60637, USA

Received December 17, 2008; Accepted February 3, 2009

DOI: 10.3892/ijo_00000282

Abstract. Regulatory T cells ($CD4^+CD25^+FoxP3^+$, Treg) have been shown to play a major role in suppression of the immune response to malignant gliomas. In this study, we investigated the kinetics of Treg infiltration in metastatic brain tumor models, including melanoma, breast and colon cancers. Our data indicate that both $CD4^+$ and Treg infiltration are significantly increased throughout the time of metastatic tumor progression. These findings were recapitulated in human CNS tumor samples of metastatic melanoma and non-small cell lung carcinoma. Collectively, these data support investigating immunotherapeutic strategies targeting Treg in metastatic CNS tumors.

Introduction

Regulatory T cells (Treg) are a subset of $CD4^+$ T cells that have been shown to suppress immune responses. While Treg are characterized by surface expression of CD25 (IL-2Rα), this marker is shared by activated T cells, thus intracellular expression of the transcription factor forkhead/winged-helix box P3 (FoxP3) has emerged as the standard marker for positively identifying Treg (1,2). Although the exact mechanism remains controversial, Treg exercise their immunosuppressive function primarily by rendering naïve conventional $CD4^+$ T cells (Tconv) anergic, i.e., suppressing the normal Tconv response following the binding of antigen to the T cell receptor (3). As previously shown, Treg have also been reported to inhibit other parts of the immune response including memory Tconv cells (4), $CD8^+$ cytotoxic T cells (5,6), natural killer cells (7,8), NKT cells (9), dendritic cells (10) and B cells (11).

Metastatic CNS tumors are the most common tumors found within the CNS, with an estimated incidence of 8.3-12 per 100,000 per year (12-14). The most common sources are lung, breast and skin (melanoma), of which nearly 10% lead to CNS metastases (15). Treg have been demonstrated to be present in increased percentages in many different primary solid tumors including lung (16), breast (17), melanoma (18,19), renal (20) and colorectal cancers (21). Previously we have demonstrated that Treg are present in primary CNS tumors (22), and that their fraction increases with tumor stage (23). However, the role of Treg in metastatic CNS tumors has not been characterized. Given the prevalence of metastatic CNS tumors and the disease burden they impose, examination of Treg in the context of these tumors is highly relevant.

In the present study, we implanted non-CNS murine tumor lines intracranially to determine whether these metastatic tumors would be infiltrated by Treg. Furthermore, we examined patient samples from human non-small cell lung carcinoma and melanoma that were metastatic to the brain. We found extensive Treg infiltration in our mouse models of metastatic melanoma, breast and colon cancer. The finding of Treg infiltration was recapitulated in the patient samples of metastatic melanoma and non-small cell lung carcinoma. To the best of our knowledge, this is the first study to show that Treg infiltrate metastatic CNS malignancies. Collectively, our data suggest that Treg targeting strategies may also be an effective treatment for certain CNS metastatic tumors.

Materials and methods

Experimental animals. Six-week old Balb/c mice were purchased from Taconic (Germantown, NY) or Jackson Labs (Bar Harbor, ME). FoxP3-GFP mice were a generous gift from A. Rudensky and have been previously characterized (2). Animals were handled in accordance with a protocol approved by the Institutional Animal Care Committee at the University of Chicago.

Cell lines. The murine melanoma cancer cell line (B16-F10) and breast cancer cell line (4T1) were obtained from American Type Culture Collection (Rockville, MD). The murine colon cancer cell line (CT26) was obtained from Dr Drew Pardoll at Johns Hopkins, Baltimore, MD and has been previously described (24). B16-F10 and 4T1 cells were cultured in 90% RPMI-1640 media with 10% FCS, 50 U/ml penicillin, 50 μg/ml streptomycin and 0.12 mg/ml L-glutamine. CT26 cells were cultured in 90% DMEM with 10% FCS, 50 U/ml penicillin, 50 μg/ml streptomycin and 0.12 mg/ml L-glutamine. All cell lines were maintained at 37˚C with 5% CO_2 in a humidified incubator.

Correspondence to: Dr Maciej S. Lesniak, The Brain Tumor Center, The University of Chicago Pritzker School of Medicine, 5841 South Maryland Ave, M/C 3026, Chicago, IL 60637, USA
E-mail: mlesniak@surgery.bsd.uchicago.edu

Key words: regulatory T cell ($CD4^+CD25^+FoxP3^+$, Treg), metastases, brain tumors, melanoma, lung cancer, colon cancer, breast cancer

Experimental intracranial tumor model. B16-F10, 4T1 and CT26 cells were cultured to 80% confluence, trypsinized, washed and resuspended in sterile PBS. B16-F10 cells ($1x10^5$), $1x10^5$ 4T1 cells or $1x10^5$ CT26 cells were prepared in 2.5 μl of PBS. In order to study these tumors in a syngeneic model, we implanted B16-F10 cells into FoxP3-GFP mice (C57BL/6 background), and 4T1 or CT26 cells were implanted into Balb/c mice. We utilized 8 mice/each experimental group.

Animals were anesthetized with an intraperitoneal injection of 0.20 ml solution of 1.25 mg/ml ketamine and 125 mg/ml xylazine in PBS. Surgical sites were shaved and prepared with providone-iodine solution. A midline incision was made in the scalp, then a 1 mm right parietal burr hole centered 2 mm posterior to the coronal suture and 2 mm lateral to the sagittal suture was made. Animals were then placed in a stereotactic frame (David Kopf Instruments, Tujunga, CA) and cells were delivered intracranially over a period of 2 min using a 25 μl Hamilton syringe (Fisher Scientific, Pittsburg, PA) via a 26 gauge needle to a depth of 3 mm from the surface of the skull. The needle was removed, the site was irrigated with sterile 0.9% NaCl, and the skin sutured.

Isolation of lymphocytes from the brain. B16-F10, CT26 and 4T1 tumor-bearing mice were sacrificed at 10, 15 and 21 days post-implantation. The mice were perfused by making a V shaped incision in the chest wall and injecting 10 ml of sterile PBS into the left ventricle. Brains were harvested and processed as described previously (25). Briefly, following mechanical disruption, cells were incubated for 30 min at 37˚C in digestion media containing collagenase D, DNAse I, HEPES, TLCK (Sigma, St. Louis, MO) in HBSS. Debris was allowed to settle for 30 min and the supernatant was collected. Cells were pelleted, resuspended in HBSS and then layered on top of a 75% Ficoll gradient. Tubes were spun at 500 x g for 30 min and the bottom layer was collected and diluted 10x with HBSS then spun at 300 x g for 10 min. The cells were resuspended in HBSS with FCS and stained for analysis by flow cytometry.

Isolation of patient tumor samples. Metastatic melanoma and non-small cell lung cancer samples were obtained directly from patients undergoing surgical resection in accordance with a protocol approved by the Institutional Review Board at the University of Chicago.

Isolation of PBMC. For mice, blood was obtained by retro-orbital sinus puncture. Red blood cells were lysed according to manufacturer's instructions with a red blood cell lysing buffer (Lonza, Allendale, NJ). PBMC were pelleted and resuspended in HBSS with FCS and stained for flow cytometric analysis. Human PBMC were isolated by layering blood over Histopaque (Sigma) and centrifuging at 400 x g for 30 min. The cells at the interface were collected and washed 3 times with HBSS prior to staining and analysis by flow cytometry.

Flow cytometry. The following antibodies were used for cell surface staining of murine cells and were purchased from BD Pharmingen (BD, San Diego, CA): PE-Cy5-CD4, FITC-CD4 and PE-CD25. The APC-FoxP3 staining was performed according to the manufacturer's kit instructions (eBioscience). Human antibodies used included FITC-CD4 (BD) and PE-FoxP3 (eBioscience). Samples were analyzed on FACs Canto (BD) and LSRII (BD). Results were analyzed in Flowjo (TreeStar, Inc., Ashland, OR). Four distinct populations were analyzed: the frequency of $CD4^+$ cells within the lymphocyte gate ($CD4^+$ T cell infiltration); the frequency of $FoxP3^+$ cells within the $CD4^+$ gate ($FoxP3^+$ fraction); the frequency of $CD4^+FoxP3^+$ cells within the lymphocyte gate (Treg infiltration); and the frequency of $CD4^+FoxP3^-$ cells within the lymphocyte gates (Tconv infiltration).

Statistical analysis. Results are expressed as mean ± standard deviation (SD). Student's t-test was used according to the distribution of experimental values. $P<0.05$ was accepted as a significant difference between groups.

Results

The kinetics of Treg infiltration in B16 melanoma of the CNS. Previous studies have shown Treg infiltration in melanomas in a B16-F10 murine flank model (26) and patient skin samples (27). To elucidate the ability of metastatic melanoma to the CNS to be infiltrated by Treg, mice were implanted with B16-F10 cells and the brains were harvested at 10, 15 and 21 days after implantation to assess the kinetics of Treg infiltration. At all time-points, the brains of tumor-bearing mice had visible tumors, and on day 21 the tumor was approximately 0.7 cm^2 and the mice showed severe symptoms of cachexia, lethargy and ataxia. No mice receiving B16-F10 tumors survived past 25 days.

The brains of the tumor-bearing mice showed biphasic kinetics of $CD4^+$ T cell infiltration, peaking at day 10, dropping sharply at day 15, and partially recovering at day 21 post-tumor implantation (Fig. 1A). In a representative mouse, on day 10 post-implantation, the tumor-bearer had increased $CD4^+$ T cell infiltration (2.67%) compared to a control mouse (0%). As the tumor progressed to day 15, mice showed a reduction in $CD4^+$ T cell infiltration (0.53%), although it remained higher than control animals. On day 21, the frequency of $CD4^+$ T cells increased to 1.76% in tumor-bearing mice.

Among $CD4^+$ cells in the tumor-bearing mice, 17.6% were $CD25^+$, of which 87.4% were $FoxP3^+$ on day 10 (Fig. 1A). In contrast, the control mouse showed no $CD4^+CD25^+$ or $CD4^+CD25^+FoxP3^+$ cells. By day 15, the frequency of $CD4^+CD25^+$ T cells increased to 29.5%. Within this $CD4^+CD25^+$ gate, 83.9% of the cells were $FoxP3^+$. The $CD4^+CD25^+$ population decreased to 9.68% on day 21, with approximately 59.4% of these cells being $FoxP3^+$.

As shown in Fig. 1B, at day 10 the frequency of $CD4^+$ $FoxP3^-$ Tconv cells in the lymphocyte gate of tumor-bearing mice was 4.16%, significantly higher than in controls (0.012%, $p=0.00060$). The frequency of Tconv cells significantly decreased to 0.22% at 15 days ($p=0.012$) and then increased significantly at 21 days (1.20%, $p=0.010$). Treg infiltration followed a similar pattern; on day 10, $CD4^+$ $FoxP3^+$ Treg (0.94%) made up a significantly higher percentage of the

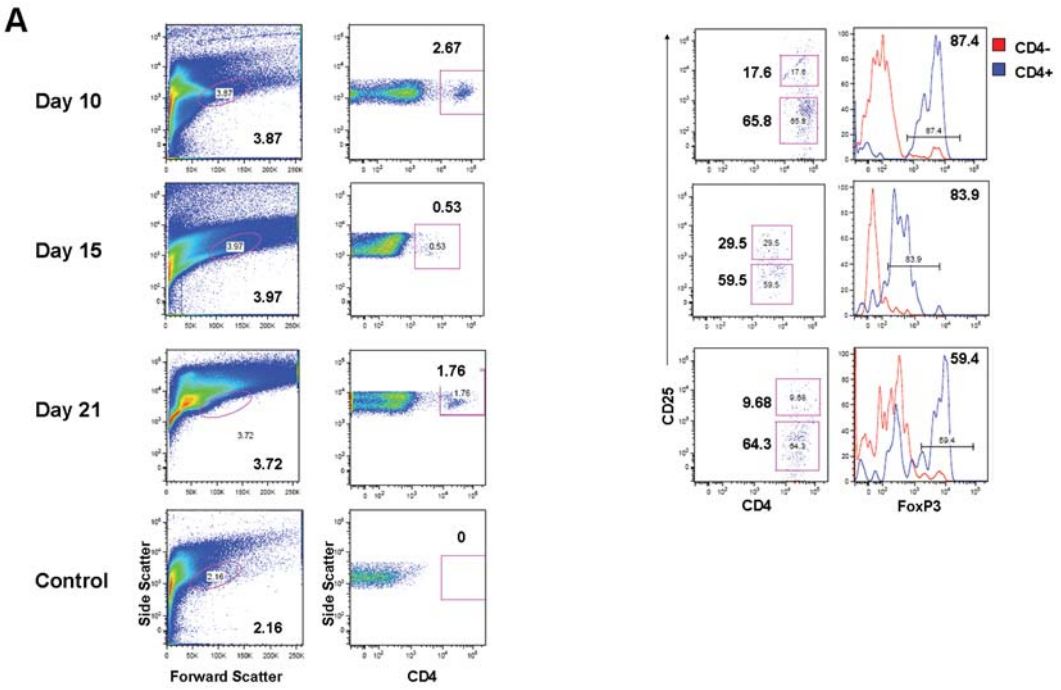

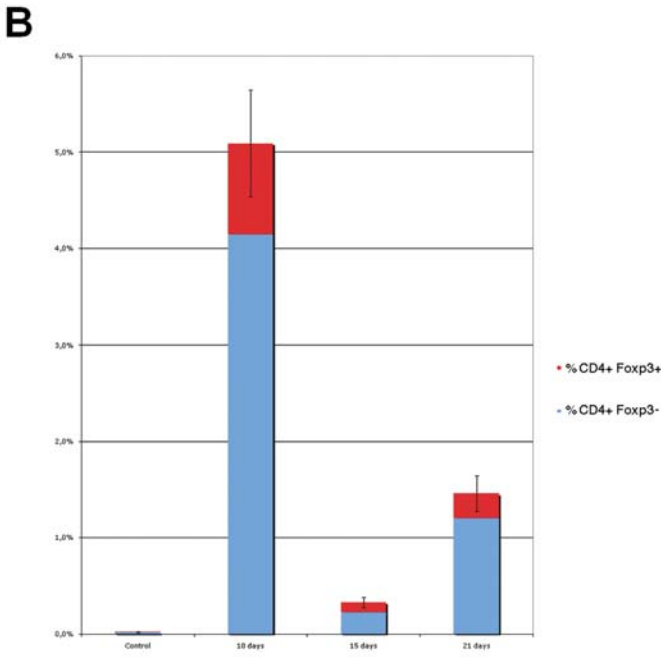

Figure 1. Flow cytometric detection of Treg in the brain in the B16 murine model of metastasis. (A) Analysis of representative B16 tumor-bearing brain sample in FoxP3-GFP mouse and control brain sample in C57BL/6 mouse, both enriched for lymphocytes on Ficoll gradient. Left panels, detection and gating of lymphocytes by side scatter and forward scatter. Second panels, detection and gating of $CD4^+$ lymphocytes. Third panels, detection and gating of $CD4^+$ lymphocytes into $CD25^+$ and $CD25^-$ fractions. Right panels, comparison of FoxP3-GFP fluorescence between $CD4^+$ $CD25^+$ and $CD4^+CD25^-$ lymphocytes. (B) Comparison of $CD4^+FoxP3^+$Treg and $CD4^+FoxP3^-$ Tconv cells in brains of control mice and B16-F10 tumor-bearing FoxP3-GFP mice harvested at 10, 15, and 21 days. Data are expressed as percentage of cells in the lymphocyte gate. Treg infiltration is the % $CD4^+$ $FoxP3^+$ cells in the lymphocyte gate. Tconv infiltration is the % of $CD4^+FoxP3^-$ cells in the lymphocyte gate. Total $CD4^+$ infiltration is the sum of Treg and Tconv infiltration. Total $CD4^+$ infiltration was significantly increased at all time points vs. controls ($p<0.05$). Total $CD4^+$ declined from 10 days to 15 days ($p=0.012$) and increased from 15 days to 21 days ($p=0.010$). Treg infiltration was significantly higher at all time points vs. controls ($p<0.05$). It was highest at 10 days after tumor implantation and declined significantly at 15 days ($p=0.022$) then increased at 21 days ($p=0.038$) but remains significantly lower than at 10 days ($p=0.011$).

lymphocyte gate than controls (0.010%, p=0.0026). The frequency of Treg decreased significantly by day 15 (0.11%, p=0.022) and on day 21 it had partially recovered to 0.29%, but was still lower than on day 10 (p=0.038). The $FoxP3^+$ fraction within the total $CD4^+$ compartment followed the opposite pattern rising significantly from day 10 (18.7%) to day 15 (31.8%) (p=0.0034), then decreasing on day 21 (17.7%) to levels similar to that of day 10 (p=0.79).

These data indicate that both Tconv and Treg infiltration are significantly increased over controls early in tumor progression and that the steepest decline in Tconv cell infiltration corresponds with the peak in the $FoxP3^+$ fraction within the $CD4^+$ compartment.

Differential $CD4^+CD25^+FoxP3^+$ Treg infiltration of intracranial breast tumors compared to colon tumors. Having examined the kinetics of Treg infiltration in the murine model of CNS metastatic melanoma, we next analyzed the ability of Treg to infiltrate two other intracranial metastases models, breast and colon cancer. We implanted 4T1 cells (breast cancer) or CT26 (colon cancer) in the brains of syngeneic Balb/c mice and assessed Treg infiltration post tumor implantation.

The time-course results with 4T1 and CT26 tumors paralleled our findings in B16-F10 melanoma model. A representative and most significant result from day 21 is shown in Fig. 2. The mouse implanted with 4T1 showed extensive $CD4^+$ T cell infiltration (3.75%) and a $CD4^+CD25^+$ fraction (8.17%) within the $CD4^+$ population. The $CD4^+$ $CD25^+$ fraction exhibited a higher percentage of $FoxP3^+$ cells than the $CD4^+CD25^-$ fraction (52.6% vs. 4.13%) (Fig. 2A).

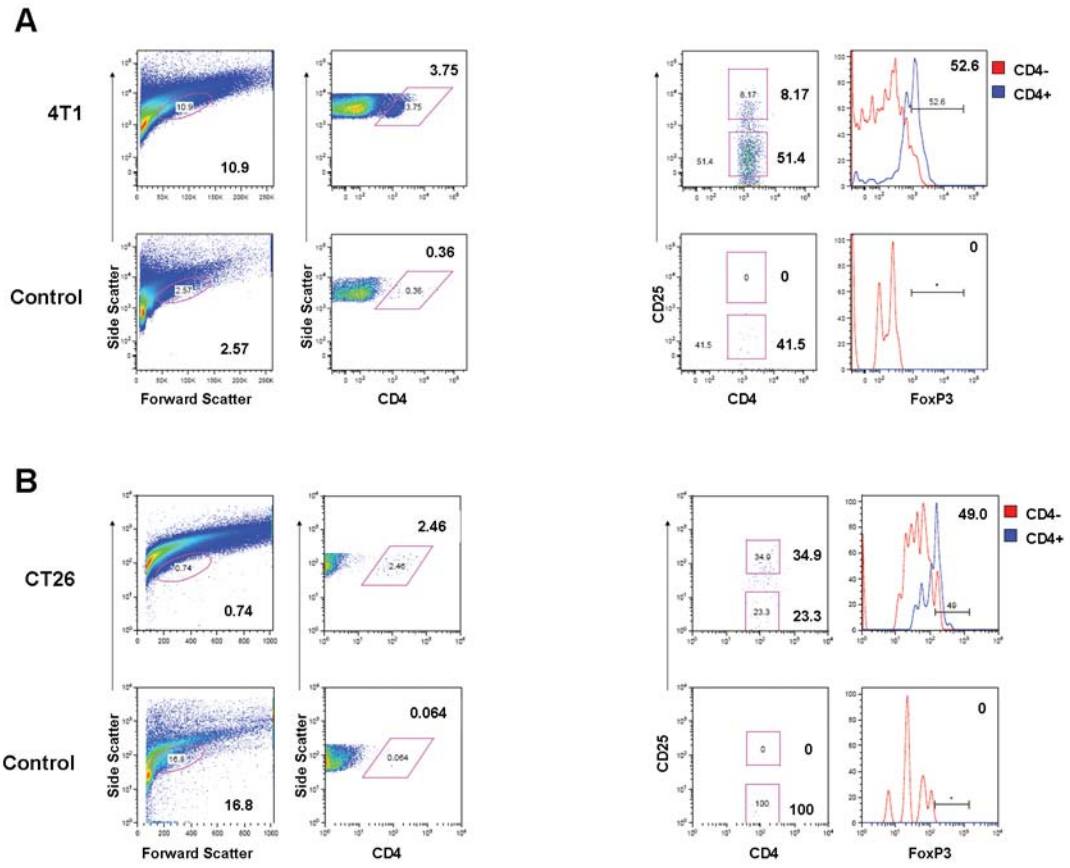

Figure 2. Flow cytometric detection of Treg in the brains of CT26 and 4T1 tumor bearing mice. Analysis of representative 4T1 (A) and CT26 (B) tumor bearing brain sample in Balb/c mouse (top) and control brain sample in Balb/c mouse (bottom), both enriched for lymphocytes on Ficoll gradient. Left panels, detection and gating of lymphocytes by side scatter and forward scatter. Second panels, detection and gating of $CD4^+$ lymphocytes. Third panels, detection and gating of $CD4^+$ lymphocytes into $CD25^+$ and $CD25^-$ fractions. Right panels, comparison of FoxP3 expression between $CD4^+CD25^+$ and $CD4^+CD25^-$ lymphocytes. (C) Comparison of $CD4^+$ $FoxP3^+$ Treg and $CD4^+$ $FoxP3^-$ Tconv infiltration in brains of control mice, CT26 and 4T1 tumor bearing mice. Data are expressed as percentage of cells in the lymphocyte gate. Treg infiltration is the % $CD4^+$ $FoxP3^+$ cells in the lymphocyte gate. Tconv infiltration is the % of $CD4^+$ $FoxP3^-$ cells in the lymphocyte gate. Total $CD4^+$ infiltration is the sum of Treg and Tconv infiltration. Treg fraction is % of Treg within the total $CD4^+$ population. $CD4^+$ infiltration was significantly higher in both CT26 (p=0.000044) and 4T1 (p=0.0028) mice vs. controls. $FoxP3^+$ fraction was significantly higher in CT26 (p=0.000071) and 4T1 (p=0.00011) vs. controls. Treg infiltration was significantly higher in CT26 (p=0.0018) and 4T1 (p=0.0024) vs. controls.

At the same time, the control brain showed significantly lower infiltration by $CD4^+$ cells (0.36%, p=0.00023), with virtually no $CD4^+CD25^+$ or $FoxP3^+$ cells.

In a representative sample from the CT26 model (Fig. 2B), the tumor-bearing brain showed extensive $CD4^+$ T cell infiltration (2.46%) in the lymphocyte gate on day 21, while the control brain showed very low infiltration (0.064%). In the tumor-bearing brain, a large percentage of $CD4^+$ cells were also $CD25^+$ (34.9%). These $CD4^+CD25^+$ cells showed higher $FoxP3^+$ expression than $CD4^+CD25^-$ cells (49% vs. 8.8%), indicating the presence of Treg and not activated $CD4^+$ T cells.

Given that we observed Treg infiltration in our syngeneic murine models of metastatic breast cancer and colon cancer, we next compared the infiltration of 4T1 and CT26 (Fig. 2C). Both 4T1 (3.43%) and CT26 (2.84%) tumor bearing mice showed significantly increased $CD4^+$ Tconv cell infiltration compared to controls (0.12%, p=0.0028 and p=0.000044). Both 4T1 (0.36%) and CT26 (1.45%) had a higher overall $CD4^+FoxP3^+$ Treg infiltration than control mice (0%, p=0.0024 and p=0.0018). The $FoxP3^+$ fraction within the $CD4^+$ compartment was elevated in 4T1 (10.7%) and CT26

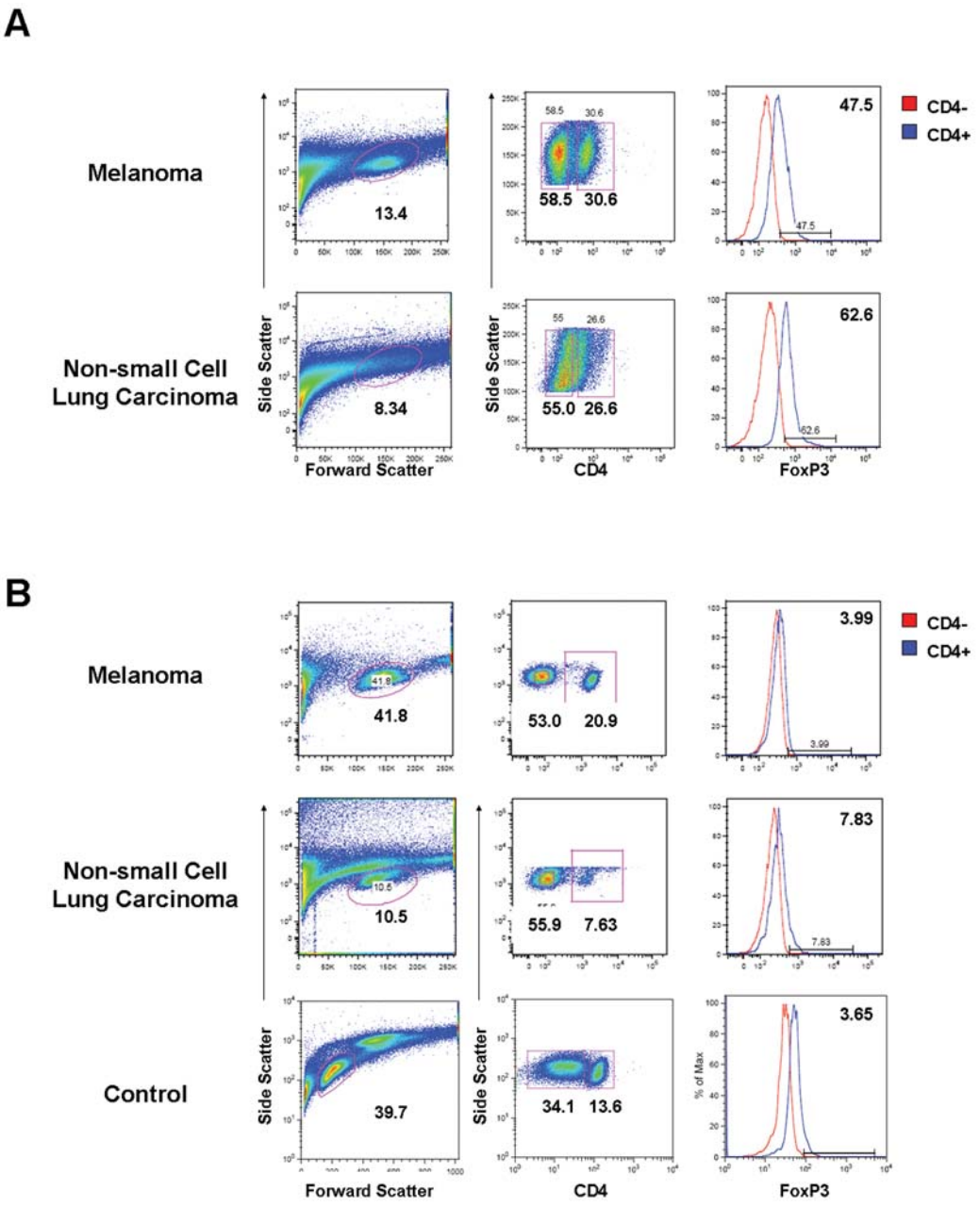

Figure 3. Flow cytometric detection of Treg in human CNS tumors in patients with metastatic melanoma and non-small cell lung cancer. (A) Analysis of CNS tumor sample from patient with metastatic melanoma and a non-small cell lung carcinoma. In a melanoma patient, we observed infiltration by CD4$^+$ cells, 47.5% of cells were FoxP3$^+$ vs. 0.94% in the CD4$^-$ gate. In the non-small cell lung carcinoma patient, we found evidence of CD4$^+$ infiltration (26.6%) and a high percentage of FoxP3$^+$ cells in the CD4$^+$ fraction (62.6% vs. 0.85% in the CD4$^-$ fraction). Our published data shows no evidence of Treg infiltration in normal human brain (22). (B) Analysis of peripheral blood from a patient with metastatic melanoma (top), a non-small cell lung carcinoma (middle), and healthy control (bottom). Left panels, detection and gating of lymphocytes by side scatter and forward scatter. Second panels, detection and gating of CD4$^+$ lymphocytes. Right panels, comparison of FoxP3 expression between CD4$^-$ and CD4$^+$ cells. Within the peripheral blood of the melanoma patient, 20.9% of the total cells were CD4$^+$, and FoxP3$^+$ fraction was 3.99%. The peripheral blood of the non-small cell lung carcinoma patient contained 7.63% CD4$^+$ cells, of which 7.83% were FoxP3$^+$. As a comparison, we tested peripheral blood from a healthy control and found 13.6% of the cells were CD4$^+$ and a FoxP3$^+$ fraction of 3.65%.

(50.0%) compared to the control mice (0%, p=0.00011 and p=0.000071). These data illustrate differential inflitraton of Treg in intracranial breast and colon cancers.

Human melanoma and non-small cell lung carcinoma show infiltration by CD4$^+$FoxP3$^+$ regulatory T cells in the CNS. Our mouse models of metastatic tumors demonstrate Treg infiltration, therefore we sought to determine the ability of human metastatic tumors to recruit Treg. To determine whether Treg are present in human CNS metastases, we analyzed two patient samples of freshly resected tumors and PBMC. In a melanoma patient, within the tumor, we observed infiltration by CD4$^+$ cells (30.6% of cells within the lymphocyte gate) (Fig. 3A). Within the CD4$^+$ gate, 47.5% of cells were FoxP3$^+$ vs. 0.94% in the CD4$^-$ gate. In the non-small cell lung carcinoma patient, we also found evidence of CD4$^+$ infiltration (26.6%) and a high percentage of FoxP3$^+$ cells in the CD4$^+$ fraction (62.6% vs. 0.85% in the CD4$^-$ fraction)

(Fig. 3A). Our published data show no evidence of Treg infiltration in normal human brain (22).

Within the peripheral blood of the melanoma patient, 20.9% of the total cells were $CD4^+$, and the $FoxP3^+$ fraction was within the expected range at 3.99% (Fig. 3B). The peripheral blood of the non-small cell lung carcinoma patient contained 7.63% $CD4^+$ cells, of which 7.83% were $FoxP3^+$. As a comparison, we tested peripheral blood from a healthy control and found 13.6% of the cells were $CD4^+$ and a $FoxP3^+$ fraction of 3.65% (Fig. 3B). These data illustrate the ability of Treg to infiltrate into metastatic CNS tumors in actual patients.

Discussion

Metastatic brain tumors represent a critical and often understudied area in the field of neuro-oncology. In one recent study of women with Her-2/neu positive breast carcinoma being treated with trastumuzab, 50% of the mortality was judged due to CNS metastases (28). Unfortunately, the treatment of CNS metastases with conventional therapy is often problematic. The blood-brain barrier often limits or blocks chemotherapeutic agents from reaching CNS lesions and the sensitivity and importance of the brain limits radiation dosages and constrains resection margins. The exquisite specificity of the immune system offers the potential for limiting collateral damage to the brain, therefore immunotherapy is often cited as a possible ideal therapy for both primary and metastatic CNS tumors.

Previously, we (22,23) and our colleagues (29,30) have demonstrated Treg infiltration in primary CNS tumors. Furthermore, the murine model of GBM suggests that Treg are actively mediating anti-tumor immunosuppression, such that selective depletion of this population leads to improved survival (29,31). Treg have been shown to play an important role in mediating anti-tumor immunosuppression in murine flank models and primary patient samples of breast (32,33) and colon tumors (34,35), non-small cell lung carcinoma (36,37), as well as melanoma (26,38,39). However, the role of Treg in CNS metastases has not been described, thus we investigated Treg infiltration in these four highly invasive CNS metastatic tumors.

Quezada and colleagues have demonstrated Treg infiltration in the murine flank model of melanoma (18). Using our CNS metastatic melanoma model, we show that early in tumor progression there is a large absolute increase in Tconv cells infiltrating the tumor, which suggests that the immune system is capable of mounting a response to the tumor. However, we also observed a corresponding increase in Treg infiltrating the tumor. Taken together, these data indicate that immune cells are able to cross the blood-brain barrier to mount an anti-tumor immune response, but the effectiveness of the immune response is likely blunted by the increased Treg fraction.

Interestingly, both the Tconv infiltration and the Treg infiltration in the metastatic melanoma tumor began on day 10, dropped precipitously at day 15, and then partially recovered on day 21. This biphasic response may represent suppression of initial Tconv cell expansion followed by the either the immune system overcoming immunosuppression due to strength of antigenic stimulation or alternatively the exhaustion of the Treg population within the tumor. While we are unsure of the reason for the decline in Treg fraction in our model, we know that it occurred too late for recovery, since at day 21 the mice show severe cachexia, lethargy and in some cases ataxia, all signs of imminent death. This is an interesting finding in light of results from Curtin and colleagues, who found that depleting Treg populations early in the tumor growth phase of a murine intracranial glioblastoma model led to a high number of long-term survivors (40). Taken together with our results, this suggests that the ideal window for Treg depletion may lie early in tumor progression, i.e., before Treg have caused significant immunosuppression and lymphopenia. This further suggests that performing clinical trials in which Treg depletion is used as a 'salvage therapy' might not be a true test of its value.

The 4T1 mammary carcinoma model has been described as a particularly challenging breast tumor model because of its tendency to metastasize early, its high lethality, and resistance to immunotherapy (41,42). In contrast, the CT26 colon cancer cell line is a chemically-induced, undifferentiated adenocarcinoma cell line, which is not highly immunogenic (43). Treg have been shown to play a key role in immunosuppression in flank models of both breast cancer (32,41) and colon cancer (44). In our syngeneic models of CNS metastatic breast and colon tumors, both showed statistically significant increases in overall $CD4^+$ T cell infiltration, Treg infiltration, as well as an increased Treg fraction within the $CD4^+$ compartment. Nonetheless, the difference in Treg infiltration between CT26 and 4T1 tumors suggests that Treg may play a differential role in immunosuppression, depending on the underlying tumor. These differences in Treg infiltration may be due to relative levels of cytokine and chemokine expression by CT26 and 4T1. Both CT26 and 4T1 have been shown to express the putative Treg chemotactic factor CCL2 (45,46) as well as the TGF-ß (47,48) and Cox-2 (49-52) which have been implicated in the conversion of Tconv into Treg (37,53,54).

Finally, the detection of an increased fraction of $CD4^+$ $FoxP3^+$ Treg in freshly resected tumor samples from patients supports our belief that these findings recapitulate the *in vivo* biology of metastatic tumors. The fact that the Treg fraction within the peripheral blood was within the expected range, while there was a high frequency within the tumor, leaves open the question of whether the source of the increased Treg fraction within the brain is due to increased recruitment, or induction of Treg from Tconv cells. Experiments by Jordan *et al* suggest that the chemokine CCL2 plays a key role in recruiting Treg to primary brain tumors (55), which is in contrast to Curiel who suggests that CCL22 drives Treg migration in ovarian carcinoma (56). Other investigators, notably Jarnicki *et al* (48) and Zhou and Levitski (57) argue that the tumor microenvironment induces the conversion of Tconv cells into Treg. Thus, the mechanism behind the increase in Treg infiltration in CNS metastases is an open question and merits further study.

Given their immunosuppressive capacity, Treg represent both an obstacle and an opportunity in designing immunotherapeutic treatments for metastatic CNS tumors. Multiple pre-clinical studies that focused on depleting Treg in primary tumors have suggested a role for these cells in

cancer immune escape. Regulatory T cell depletion has resulted in increased survival times (31,58), increased immune responses to tumors (59), enhanced response to immunotherapy (60) and in some combinations led to tumor rejection (26,61). Early experiments in humans have yielded mixed results, with some investigators reporting that some measures of immune response are improved following Treg depletion (62-64) while others report disappointing results (65). Multiple clinical trials exploring different approaches to combining Treg depletion with other immunotherapy strategies are ongoing. Given our results it seems reasonable that future immunotherapeutic strategies directed at metastatic CNS lesions might explore adjunctive therapies to target Treg.

In conclusion, we show that $CD4^+CD25^+FoxP3^+$ Treg are present in four common CNS metastases. We detected elevated Treg fractions in murine models of melanoma, breast cancer and colon cancer, as well as in CNS tumor samples from patients with metastatic human non-small cell lung cancer and melanoma. While the presence of high concentrations of Treg in CNS metastases may present an obstacle to inducing immune responses, Treg represent a potential target. Future studies should be aimed at evaluating the effectiveness of depleting Treg in CNS metastases.

Acknowledgements

We thank the staff at the University of Chicago flow cytometry facility for their assistance, particularly Ryan Duggan, David Leclerc, and Michael Olson. This study was supported by the National Institutes of Health and the National Cancer Institute (R01-CA138587; MSL).

References

1. Hori S, Nomura T and Sakaguchi S: Control of regulatory T cell development by the transcription factor Foxp3. Science 299: 1057-1061, 2003.
2. Fontenot JD, Rasmussen JP, Williams LM, *et al*: Regulatory T cell lineage specification by the forkhead transcription factor foxp3. Immunity 22: 329-341, 2005.
3. Takahashi T, Kuniyasu Y, Toda M, *et al*: Immunologic self-tolerance maintained by $CD25^+CD4^+$ naturally anergic and suppressive T cells: induction of autoimmune disease by breaking their anergic/suppressive state. Int Immunol 10: 1969-1980, 1998.
4. Levings MK, Sangregorio R and Roncarolo MG: Human cd25(+)cd4(+) t regulatory cells suppress naive and memory T cell proliferation and can be expanded in vitro without loss of function. J Exp Med 193: 1295-1302, 2001.
5. Piccirillo CA and Shevach EM: Cutting edge: control of $CD8^+$ T cell activation by $CD4^+CD25^+$ immunoregulatory cells. J Immunol 167: 1137-1140, 2001.
6. Suvas S, Kumaraguru U, Pack CD, *et al*: $CD4^+CD25^+$ T cells regulate virus-specific primary and memory $CD8^+$ T cell responses. J Exp Med 198: 889-901, 2003.
7. Smyth MJ, Teng MW, Swann J, *et al*: $CD4^+CD25^+$ T regulatory cells suppress NK cell-mediated immunotherapy of cancer. J Immunol 176: 1582-1587, 2006.
8. Ghiringhelli F, Menard C, Terme M, *et al*: $CD4^+CD25^+$ regulatory T cells inhibit natural killer cell functions in a transforming growth factor-beta-dependent manner. J Exp Med 202: 1075-1085, 2005.
9. Azuma T, Takahashi T, Kunisato A, *et al*: Human $CD4^+$ $CD25^+$ regulatory T cells suppress NKT cell functions. Cancer Res 63: 4516-4520, 2003.
10. Misra N, Bayry J, Lacroix-Desmazes S, *et al*: Cutting edge: human $CD4^+CD25^+$ T cells restrain the maturation and antigen-presenting function of dendritic cells. J Immunol 172: 4676-4680, 2004.
11. Zhao DM, Thornton AM, DiPaolo RJ, *et al*: Activated $CD4^+CD25^+$ T cells selectively kill B lymphocytes. Blood 107: 3925-3932, 2006.
12. Walker AE, Robins M and Weinfeld FD: Epidemiology of brain tumors: the national survey of intracranial neoplasms. Neurology 35: 219-226, 1985.
13. Percy AK, Elveback LR, Okazaki H, *et al*: Neoplasms of the central nervous system. Epidemiologic considerations. Neurology 22: 40-48, 1972.
14. Kehrli P: [Epidemiology of brain metastases]. Neurochirurgie 45: 357-363, 1999.
15. Barnholtz-Sloan JS, Sloan AE, Davis FG, *et al*. Incidence proportions of brain metastases in patients diagnosed (1973 to 2001) in the Metropolitan Detroit Cancer Surveillance System. J Clin Oncol 22: 2865-2872, 2004.
16. Woo EY, Chu CS, Goletz TJ, *et al*: Regulatory CD4(+)CD25(+) T cells in tumors from patients with early-stage non-small cell lung cancer and late-stage ovarian cancer. Cancer Res 61: 4766-4772, 2001.
17. Liyanage UK, Moore TT, Joo HG, *et al*: Prevalence of regulatory T cells is increased in peripheral blood and tumor microenvironment of patients with pancreas or breast adenocarcinoma. J Immunol 169: 2756-2761, 2002.
18. Quezada SA, Peggs KS, Curran MA, *et al*: CTLA4 blockade and GM-CSF combination immunotherapy alters the intratumor balance of effector and regulatory T cells. J Clin Invest 116: 1935-1945, 2006.
19. Viguier M, Lemaitre F, Verola O, *et al*: Foxp3 expressing $CD4^+$CD25(high) regulatory T cells are overrepresented in human metastatic melanoma lymph nodes and inhibit the function of infiltrating T cells. J Immunol 173: 1444-1453, 2004.
20. Cesana GC, DeRaffele G, Cohen S, *et al*: Characterization of $CD4^+CD25^+$ regulatory T cells in patients treated with high-dose interleukin-2 for metastatic melanoma or renal cell carcinoma. J Clin Oncol 24: 1169-1177, 2006.
21. Ling KL, Pratap SE, Bates GJ, *et al*: Increased frequency of regulatory T cells in peripheral blood and tumour infiltrating lymphocytes in colorectal cancer patients. Cancer Immun 7: 7, 2007.
22. El Andaloussi A and Lesniak MS: An increase in $CD4^+$ $CD25^+FOXP3^+$ regulatory T cells in tumor-infiltrating lymphocytes of human glioblastoma multiforme. Neuro Oncol 8: 234-243, 2006.
23. El Andaloussi A and Lesniak MS: $CD4^+$ $CD25^+$ $FoxP3^+$ T-cell infiltration and heme oxygenase-1 expression correlate with tumor grade in human gliomas. J Neurooncol 83: 145-152, 2007.
24. Brattain MG, Strobel-Stevens J, Fine D, *et al*: Establishment of mouse colonic carcinoma cell lines with different metastatic properties. Cancer Res 40: 2142-2146, 1980.
25. Walker PR, Calzascia T, Schnuriger V, *et al*: The brain parenchyma is permissive for full antitumor CTL effector function, even in the absence of CD4 T cells. J Immunol 165: 3128-3135, 2000.
26. Kline J, Brown IE, Zha YY, *et al*: Homeostatic proliferation plus regulatory T-cell depletion promotes potent rejection of b16 melanoma. Clin Cancer Res 14: 3156-3167, 2008.
27. Miracco C, Mourmouras V, Biagioli M, *et al*: Utility of tumour-infiltrating $CD25^+FOXP3^+$ regulatory T cell evaluation in predicting local recurrence in vertical growth phase cutaneous melanoma. Oncol Rep 18: 1115-1122, 2007.
28. Bendell JC, Domchek SM, Burstein HJ, *et al*: Central nervous system metastases in women who receive trastuzumab-based therapy for metastatic breast carcinoma. Cancer 97: 2972-2977, 2003.
29. Fecci PE, Sweeney AE, Grossi PM, *et al*: Systemic anti-CD25 monoclonal antibody administration safely enhances immunity in murine glioma without eliminating regulatory T cells. Clin Cancer Res 12: 4294-4305, 2006.
30. Hussain SF, Yang D, Suki D, Aldape K, *et al*: The role of human glioma-infiltrating microglia/macrophages in mediating antitumor immune responses. Neuro Oncol 8: 261-279, 2006.
31. El Andaloussi A, Han Y and Lesniak MS: Prolongation of survival following depletion of $CD4^+CD25^+$ regulatory T cells in mice with experimental brain tumors. J Neurosurg 105: 430-437, 2006.
32. Chaput N, Darrasse-Jeze G, Bergot AS, *et al*: Regulatory T cells prevent CD8 T cell maturation by inhibiting CD4 Th cells at tumor sites. J Immunol 179: 4969-4978, 2007.

33. Ohara M, Yamaguchi Y, Matsuura K, *et al*: Possible involvement of regulatory T cells in tumor onset and progression in primary breast cancer. Cancer Immunol Immunother (In press).
34. Loddenkemper C, Schernus M, Noutsias M, *et al*: In situ analysis of FOXP3$^+$ regulatory T cells in human colorectal cancer. J Transl Med 4: 52, 2006.
35. Ghiringhelli F, Larmonier N, Schmitt E, *et al*: CD4$^+$CD25$^+$ regulatory T cells suppress tumor immunity but are sensitive to cyclophosphamide which allows immunotherapy of established tumors to be curative. Eur J Immunol 34: 336-344, 2004.
36. Petersen RP, Campa MJ, Sperlazza J, *et al*: Tumor infiltrating Foxp3$^+$ regulatory T-cells are associated with recurrence in pathologic stage I NSCLC patients. Cancer 107: 2866-2872, 2006.
37. Sharma S, Yang SC, Zhu L, *et al*: Tumor cyclooxygenase-2/prostaglandin E2-dependent promotion of FOXP3 expression and CD4$^+$ CD25$^+$ T regulatory cell activities in lung cancer. Cancer Res 65: 5211-5220, 2005.
38. Turk MJ, Guevara-Patino JA, Rizzuto GA, *et al*: Concomitant tumor immunity to a poorly immunogenic melanoma is prevented by regulatory T cells. J Exp Med 200: 771-782, 2004.
39. Appay V, Jandus C, Voelter V, *et al*: New generation vaccine induces effective melanoma-specific CD8$^+$ T cells in the circulation but not in the tumor site. J Immunol 177: 1670-1678, 2006.
40. Curtin JF, Candolfi M, Fakhouri TM, *et al*: Treg depletion inhibits efficacy of cancer immunotherapy: implications for clinical trials. PLoS ONE 3: E1983, 2008.
41. Chen L, Huang TG, Meseck M, *et al*: Rejection of metastatic 4T1 breast cancer by attenuation of Treg cells in combination with immune stimulation. Mol Ther 15: 2194-2202, 2007.
42. Pulaski BA, Terman DS, Khan S, *et al*: Cooperativity of Staphylococcal aureus enterotoxin B superantigen, major histocompatibility complex class II, and CD80 for immunotherapy of advanced spontaneous metastases in a clinically relevant postoperative mouse breast cancer model. Cancer Res 60: 2710-2715, 2000.
43. Belnap LP, Cleveland PH, Colmerauer ME, *et al*: Immunogenicity of chemically induced murine colon cancers. Cancer Res 39: 1174-1179, 1979.
44. Golgher D, Jones E, Powrie F, *et al*: Depletion of CD25+ regulatory cells uncovers immune responses to shared murine tumor rejection antigens. Eur J Immunol 32: 3267-3275, 2002.
45. Sharma S, Karakousis CP, Takita H, *et al*: Cytokines and chemokines are expressed at different levels in small and large murine colon-26 tumors following intratumoral injections of CpG ODN. Neoplasia 6: 523-528, 2004.
46. Vitiello PF, Shainheit MG, Allison EM, *et al*: Impact of tumor-derived CCL2 on T cell effector function. Immunol Lett 91: 239-245, 2004.
47. Kobie JJ, Wu RS, Kurt RA, *et al*: Transforming growth factor beta inhibits the antigen-presenting functions and antitumor activity of dendritic cell vaccines. Cancer Res 63: 1860-1864, 2003.
48. Jarnicki AG, Lysaght J, Todryk S, *et al*: Suppression of antitumor immunity by IL-10 and TGF-beta-producing T cells infiltrating the growing tumor: influence of tumor environment on the induction of CD4$^+$ and CD8$^+$ regulatory T cells. J Immunol 177: 896-904, 2006.
49. Soslow RA, Dannenberg AJ, Rush D, *et al*: COX-2 is expressed in human pulmonary, colonic, and mammary tumors. Cancer 89: 2637-2645, 2000.
50. Takahashi T, Baba M, Nishino H, *et al*: Cyclooxygenase-2 plays a suppressive role for induction of apoptosis in isoliquiritigenin-treated mouse colon cancer cells. Cancer Lett 231: 319-325, 2006.
51. Connolly EM, Harmey JH, O'Grady T, *et al*: Cyclo-oxygenase inhibition reduces tumour growth and metastasis in an orthotopic model of breast cancer. Br J Cancer 87: 231-237, 2002.
52. Pozzi A, Yan X, Macias-Perez I, *et al*: Colon carcinoma cell growth is associated with prostaglandin E2/EP4 receptor-evoked ERK activation. J Biol Chem 279: 29797-29804, 2004.
53. Liu VC, Wong LY, Jang T, *et al*: Tumor evasion of the immune system by converting CD4$^+$CD25$^-$ T cells into CD4$^+$CD25$^+$ T regulatory cells: role of tumor-derived TGF-beta. J Immunol 178: 2883-2892, 2007.
54. Baratelli F, Lin Y, Zhu L, *et al*: Prostaglandin E2 induces FOXP3 gene expression and T regulatory cell function in human CD4$^+$ T cells. J Immunol 175: 1483-1490, 2005.
55. Jordan JT, Sun W, Hussain SF, *et al*: Preferential migration of regulatory T cells mediated by glioma-secreted chemokines can be blocked with chemotherapy. Cancer Immunol Immunother 57: 123-131, 2008.
56. Curiel TJ, Coukos G, Zou L, *et al*: Specific recruitment of regulatory T cells in ovarian carcinoma fosters immune privilege and predicts reduced survival. Nat Med 10: 942-949, 2004.
57. Zhou G and Levitsky HI: Natural regulatory T cells and de novo-induced regulatory T cells contribute independently to tumor-specific tolerance. J Immunol 178: 2155-2162, 2007.
58. Viehl CT, Moore TT, Liyanage UK, *et al*: Depletion of CD4$^+$CD25$^+$ regulatory T cells promotes a tumor-specific immune response in pancreas cancer-bearing mice. Ann Surg Oncol 13: 1252-1258, 2006.
59. Shimizu J, Yamazaki S and Sakaguchi S: Induction of tumor immunity by removing CD25$^+$CD4$^+$ T cells: a common basis between tumor immunity and autoimmunity. J Immunol 163: 5211-5218, 1999.
60. Kottke T, Galivo F, Wongthida P, *et al*: Treg Depletion-enhanced IL-2 treatment facilitates therapy of established tumors using systemically delivered oncolytic virus. Mol Ther (In press).
61. Onizuka S, Tawara I, Shimizu J, *et al*: Tumor rejection by in vivo administration of anti-CD25 (interleukin-2 receptor alpha) monoclonal antibody. Cancer Res 59: 3128-3133, 1999.
62. Morse MA, Hobeika AC, Osada T, *et al*: Depletion of human regulatory T cells specifically enhances antigen specific immune responses to cancer vaccines. Blood (In press).
63. Mahnke K, Schonfeld K, Fondel S, *et al*: Depletion of CD4$^+$CD25$^+$ human regulatory T cells in vivo: kinetics of Treg depletion and alterations in immune functions in vivo and in vitro. Int J Cancer 120: 2723-2733, 2007.
64. Dannull J, Su Z, Rizzieri D, *et al*: Enhancement of vaccine-mediated antitumor immunity in cancer patients after depletion of regulatory T cells. J Clin Invest 115: 3623-3633, 2005.
65. Powell DJ Jr, Felipe-Silva A, Merino MJ, *et al*: Administration of a CD25-directed immunotoxin, LMB-2, to patients with metastatic melanoma induces a selective partial reduction in regulatory T cells in vivo. J Immunol 179: 4919-4928, 2007.